

Challenges in Predicting $\Delta_{\text{rxn}}G$ in Solution: The Mechanism of Ether-Catalyzed Hydroboration of Alkenes

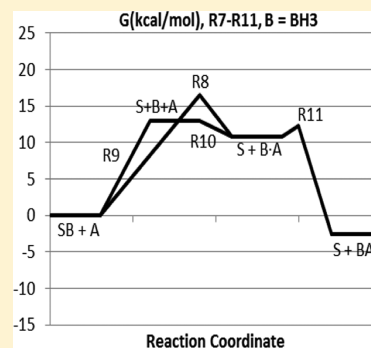
Daniel J. S. Sandbeck,[†] Colin M. Kuntz,[†] Christine Luu,[†] Rachelle A. Mondor,[†] John G. Ottaviano,[†] Aravind V. Rayer,[‡] Kazi Z. Sumon,[‡] and Allan L. L. East^{†,*}

[†]Department of Chemistry and Biochemistry, University of Regina, 3737 Wascana Parkway, Regina, SK S4S 0A2, Canada

[‡]Department of Industrial Systems Engineering, University of Regina, 3737 Wascana Parkway, Regina, SK S4S 0A2, Canada

S Supporting Information

ABSTRACT: Ab initio (coupled-cluster and density-functional) calculations of Gibbs reaction energies in solution, with new entropy-of-solvation damping terms, were performed for the ether-catalyzed hydroboration of alkenes. The goal was to test the accuracy of continuum-solvation models for reactions of neutral species in nonaqueous solvents, and the hope was to achieve an accuracy sufficient to address the mechanism in the “Pasto case”: B_2H_6 + alkene in THF solvent. Brown’s $\text{S}_{\text{N}}2/\text{S}_{\text{N}}1$ “dissociative” mechanism, of $\text{S}_{\text{N}}2$ formation of borane–ether adducts followed by $\text{S}_{\text{N}}1$ alkene attack, was at odds with Pasto’s original $\text{S}_{\text{N}}2/\text{S}_{\text{N}}2$ hypothesis, and while Brown could prove his mechanism for a variety of cases, he could not perform the experimental test with THF adducts in THF solvent, where the higher THF concentrations might favor an $\text{S}_{\text{N}}2$ second step. Two diboranes were tested: B_2H_6 , used by Pasto, and $(9\text{BBN})_2$ ($9\text{BBN} = 9\text{-borabicyclo}[3.3.1]\text{nonane}$, $\text{C}_8\text{H}_{15}\text{B}$), used by Brown. The new entropy terms resulted in improved accuracy vs traditional techniques ($\sim 2 \text{ kcal mol}^{-1}$), but this accuracy was not sufficient to resolve the mechanism in the Pasto case.



1. INTRODUCTION

Hydroboration is the addition of a B—H bond of a borane or organoborane across an unsaturated multiple bond. It is an important tool in organic synthesis, particularly for the regioselective functionalization of C=C bonds.¹

In the gas phase and in noncomplexing hydrocarbon solvents, boranes generally appear as H-bridged dimers, $(\text{BR}_2\text{H})_2$ (denoted more simply as “ B_2 ” in this paper). Their dissociation equilibria lie heavily to the left. Switching to complexing solvents, particularly ethers such as tetrahydrofuran (THF, $\text{C}_4\text{H}_8\text{O}$), the rate of hydroboration of alkenes by boranes is significantly increased.² To explain the catalytic effect of ethers, Nobel prizewinner H. C. Brown demonstrated the existence of an intermediate (here denoted SB) involving an adduct of nucleophilic solvent S to borane monomer B.² In the case of $(\text{BH}_3)_2$ + THF, the adduct intermediate is even more stable than the diborane.^{3,4} The catalytic effect required Brown to take the view that the initial adduct-forming stage (solvolysis of diboranes) must be bimolecular ($\text{S}_{\text{N}}2$, dimer + solvent), but he felt the ensuing alkene-addition stage (hydroboration of alkene) would involve $\text{S}_{\text{N}}1$ dissociation of the adduct before addition of organoborane monomer to alkene. In this regard he questioned the conclusions of Pasto,³ who for the case of THF· BH_3 argued that the second stage was also bimolecular ($\text{S}_{\text{N}}2$, adduct + alkene). Brown demonstrated the $\text{S}_{\text{N}}1$ nature of alkene addition with two different BH_3 adducts (with Et_3N and Me_2S) in toluene,⁵ but not with ethers in ether. Since an increase in ether concentration would improve the $\text{S}_{\text{N}}2$ rate vis-à-vis the $\text{S}_{\text{N}}1$ rate, it may be an open question whether

the mechanism of alkene addition is still $\text{S}_{\text{N}}1$ in THF solvent. We wished to test both of Brown’s claims ($\text{S}_{\text{N}}2$ solvolysis and $\text{S}_{\text{N}}1$ alkene-addition) for THF-solvated systems, using quantum chemistry methods.

Computationally, the first stage (solvolysis of diboranes) has been studied, but not with THF. Studies of B_2H_6 reacting with several small molecules (NH_3 ,⁶ H_2S ,⁷ and H_2O ⁸) have predicted a two-step reaction with a singly H-bridged dimer adduct intermediate, e.g. $\text{H}_3\text{NBH}_2(\text{H})\text{BH}_3$. The equivalent intermediate with THF solvent has apparently not been investigated. The solvolysis stage is also useful for calibrating the accuracy of ΔG computation methods, as Brown provided both rate and equilibrium constant data for it.² The second stage (alkene addition) has drawn interest from computational chemists^{9–13} mainly because this step determines the anti-Markovnikov product distributions. These works have predicted a minor intermediate in this stage as well: a π complex of alkene to the borane (via the empty p orbital on boron). Regarding the Brown vs Pasto issue in the second stage, in 1983 Schleyer and co-workers⁹ argued for a Pasto $\text{S}_{\text{N}}2$ alkene addition, but based on a Hartree–Fock-optimized “ $\text{S}_{\text{N}}2$ ” transition state that is rather loose, and a later computational study reported by Houk and co-workers¹⁰ in 1990 seemed inconclusive on this issue. As recently as 2008, Oyola and Singleton¹¹ (in a paper concerned with the anti-Markovnikov product distribution) commented

Received: August 1, 2014

Revised: October 24, 2014

Published: December 3, 2014



on the lingering doubt in THF solution, tentatively siding with Brown; they performed a side calculation that showed the S_N2 free energy barrier to be 2.3 kcal mol⁻¹ larger than the S_N1 dimer-dissociation free energy barrier, but they placed more weight on experimental results in siding with Brown.

We were curious to know if 2.3 kcal mol⁻¹ accuracy could be achieved from quantum chemistry methods in predicting S_N1 vs S_N2 barriers in THF solution, and thus obtain a more definitive answer regarding the mechanism in the Pasto case. We set this as the main goal of our project. A secondary goal was to confirm, via *ab initio* prediction, the utility of the spectral signatures Brown used in identifying intermediates. In the computations, THF (C₄H₈O) was the solvent *S*, isobutene (C₄H₈) was the alkene, and two different choices were made for the borane BR₂H: the simple borane BH₃ (used by Pasto^{3,4}) and “9BBN” (9-borabicyclo[3.3.1]nonane, C₈H₁₅B, used by Brown in his solvolysis study²). The project exposed several underappreciated issues in computing free energy of solvation. An improved method of calculating entropies of solvation was needed to improve accuracy over the traditional “compressed gas” approximation (see the next section), and although the target accuracy of ± 2 kcal mol⁻¹ for these reactions was achieved in the three quantitative “comparisons” presented here, this accuracy was not sufficient to resolve all mechanism issues.

2. COMPUTATIONAL METHODS

Using Gaussian03 and Gaussian09,¹⁴ three density-functional theory (DFT) methods (B3LYP,^{15,16} PBEPBE,^{17,18} and OLYP¹⁹) and three basis sets (6-31G(d), 6-31G(d,p), and cc-pVDZ)¹⁴ were tested with geometry optimization calculations. After testing, the B3LYP/6-31G(d) structures were used in all ensuing calculations.

Only the lowest-energy forms were used; this required conformer studies for 9BBN, (9BBN)₂, and THF (Figure 1). For 9BBN all levels of theory produced the same lowest-energy form (dd C_s) with a mild distortion from ideal C_{2v} symmetry. For (9BBN)₂ the optimal form (dd,dd D_{2h}) was fully symmetric at all levels of theory. For THF, the lowest-energy form was puckered,²⁰ but its symmetry was dependent on the level of theory used (C_s with PBEPBE, C₁ with OLYP, and C₂ with B3LYP); the energies of the C_s, C₁, and C₂ puckered structures all lie within 0.15 kcal mol⁻¹ of each other along a low-frequency pseudorotation mode. The INT=ULTRAFINE integration grid¹⁴ was used for THF only.

For ¹¹B-NMR calculations, single-point B3LYP/6-311+G(d,p)//B3LYP/6-31G(d) calculations using the gauge-including

atomic orbital (GIAO) method^{21,22} were employed. The absolute chemical shifts were converted to shifts relative to that of the lowest-energy conformer of the BF₃·OEt₂ adduct, which (in a conformer search) turned out to be the one having dihedral BOCC angles of -95.5° and -72.0°.

The Gibbs energies used in this paper were generated as follows. For each compound, the routine gas-phase ideal-gas rigid-rotor/harmonic-oscillator (RRHO) value was calculated, based on B3LYP/6-31G(d) electronic energies, vibrational frequencies, and rotational moments of inertia. Call this $G_{\text{gas,init}}$:

$$G_{\text{gas,init}} = E_{\text{elec}} + \delta_{\text{ZPVE}}E + \delta_{\text{T}}E + PV - TS$$

where $\delta_{\text{ZPVE}}E$ is half the sum of (unscaled) B3LYP/6-31G(d) vibrational harmonic frequencies, $\delta_{\text{T}}E$ is the RRHO thermal correction for internal energy E at $p = 1$ atm and $T = 298.15$ K, PV is taken as RT , and S is the RRHO computation of entropy. To convert $G_{\text{gas,init}}$ into a free energy of a mole of solute in solution (G_{solv}), several additive corrections could be considered (Table 1), in the same spirit as the focal-point method for improved E_{elec} values.^{23,24}

In Table 1, the first eight terms are corrections for a more accurate gas-phase Gibbs energy value. For $\delta_{\text{corr}}E$ the correction $E_{\text{elec}}[\text{CCSD(T)}/\text{cc-pVDZ}]/\text{B3LYP}/6-31\text{G(d)} - E_{\text{elec}}[\text{B3LYP}/6-31\text{G(d)}]$ was used; the CCSD(T) (coupled-cluster²⁵) calculations were performed with MOLPRO2008.²⁶ For $\delta_{\text{basis}}E$ the correction $E_{\text{elec}}[\text{B3LYP}/\text{aug-cc-pVTZ}]/\text{B3LYP}/6-31\text{G(d)} - E_{\text{elec}}[\text{B3LYP}/\text{cc-pVDZ}]$ was used. For terms 3 and 4, $\delta_{\text{anharm}}E$ might be important for reactions which break several bonds (e.g., atomization) and can be treated by frequency scaling,²⁷ while $\delta_{\text{anharm}}TS$ might be important for internal-rotation modes of molecules displaying particularly low harmonic frequencies (indicating high-entropy nearly free internal rotation) and can be treated by the E1, E2, or E3 methods published by East and Radom in 1997.²⁸ Here we computed E1 corrections for term 4 but the results were negligible and were not used (see Appendix A). For terms 5 and 6, relevant to large floppy molecules with many internal rotation modes, $\delta_{\text{conf}}E$ could be handled by Boltzmann weighting, while $\delta_{\text{conf}}TS$ could be handled by statistical counting.^{29,30}

Terms 7 and 8 ($\delta_{\text{FES}}E$ and $\delta_{\text{FES}}TS$) correct for errors due to computing G at stationary points on the potential energy surface (PES) instead of the free energy surface (FES). They are probably negligible terms except for the Gibbs energy of transition states (G^\ddagger) of bond breaking/forming reactions. Consideration of this proper Gibbs maximum is termed variational transition-state theory (vTST), and improves agreement

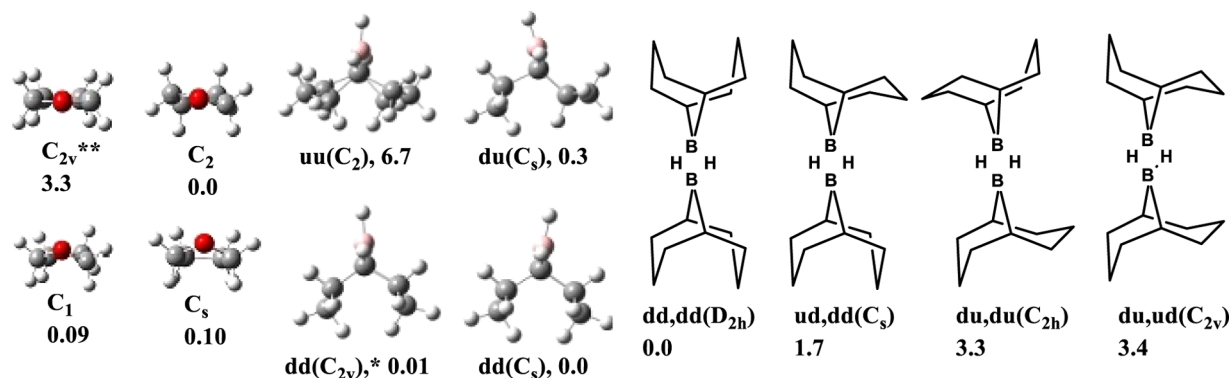


Figure 1. Conformers of THF, 9BBN, and (9BBN)₂, with B3LYP/6-31G(d) relative energies in kcal mol⁻¹. Asterisks indicate the number of imaginary frequencies according to B3LYP/6-31G(d).

Table 1. Additive Corrections To Convert B3LYP/6-31G(d) $G_{\text{gas,init}}$ Computation to G_{solv}

term ^a	label	description	used in this work
1	$\delta_{\text{corr}}E$	electron correlation correction to E_{elec}	yes
2	$\delta_{\text{basis}}E$	basis set correction to E_{elec}	yes
3	$\delta_{\text{anharm}}E$	anharmonic correction to E	no
4	$\delta_{\text{anharm}}TS$	anharmonic correction to TS	no ^c
5	$\delta_{\text{conf}}E$	correction to E for multiple conformers	no
6	$\delta_{\text{conf}}TS$	correction to TS for multiple conformers	no
7	$\delta_{\text{FES}}E$	free-energy-surface geometry-shift correction to E^b	no
8	$\delta_{\text{FES}}TS$	free-energy-surface geometry-shift correction to TS^b	yes
I	$\delta_{\text{Hbond}}E$	solute-to-solvent H bonding (if present)	no
II	$\delta_{\text{polz}}E$	solute-to-solvent dipole interaction, incl. polarization	yes
III	$\delta_{\text{disp}}E$	solute-to-solvent dispersion-attraction	no
IV	$\delta_{\text{cav}}E$	cavitation of the solvent	no
V	$\delta_{\text{reor}}E$	correction to E_{system} for solvent reordering	no
VI	$\delta_{\text{reor}}TS$	correction to TS_{system} for solvent reordering	no
VII	$\delta_{\text{damp}}PV$	damping of PV	yes
VIII	$\delta_{\text{damp}}TS_{\text{trans}}$	damping of TS_{trans}	yes
IX	$\delta_{\text{damp}}TS_{\text{rot}}$	damping of TS_{rot}	yes

^aSolvation terms listed with Roman numerals. ^bNormally only important for certain transition states (variational transition-state theory). ^cTested but not used due to negligible results.

with data from experimental rate constants.³¹ (For the alkene-addition stage, Singleton considered this Gibbs energy maximum in his dynamical investigation of product distributions.¹¹) In solution, given other approximations, $\delta_{\text{FES}}E$ and $\delta_{\text{FES}}TS$ were only deemed important in the case of “barrierless” bond associations and dissociations, where the PES has its maximum only at separated fragments; for G^\ddagger computation the free energy maximum is not at separated fragments, but at locations where the entropy is more restricted (3–4 Å in the gas phase for bonds between second period atoms). In the association direction of a “barrierless” reaction, this would be a purely entropic barrier. Since G^\ddagger prediction for barrierless reactions was needed in this project, we estimated and used $\delta_{\text{FES}}E$ and $\delta_{\text{FES}}TS$ shifts of −1.6 and −3.4 kcal mol^{−1} (i.e., $\delta_{\text{FES}}G = +1.8$ kcal mol^{−1}) for G^\ddagger for “barrierless” dissociations in THF (see Appendix B). (Note that our reported Gibbs energy profiles and $\Delta_{\text{rxn}}G^\circ$ values do not include $\delta_{\text{FES}}G$ corrections.)

The remaining nine corrections are for the act of solvation, of which we ignored five, arguing that the “non-electrostatic” terms $\delta_{\text{disp}}E$ and $\delta_{\text{cav}}E$ contribute little to $\Delta_{\text{rxn}}E$, that no H-bonds can exist between these solutes and THF, and that the solvent-reordering terms would be minor because the THF cannot H-bond to itself and is thus not a strongly ordered liquid (as a counterexample, the hydrophobic effect of nonpolar solutes in water involves large solvent-reordering terms). Of the four terms employed (II, VII, VIII, IX), we used Gaussian’s polarizable continuum model (PCM)^{32,33} for II and damping terms for PV (VII) and entropy (VIII and IX). Entropy-damping terms are rarely invoked, except perhaps in the protein-folding community,^{34,35} and therefore warrant some discussion.

As Henchman explains,³⁵ use of solute entropy damping terms constitutes one of two conventions one could use for defining Gibbs energy in solution. He terms this convention the “system-frame” (SF) convention and notes that it gives entropies of

association in solution that correspond better to experimentally derived values than the usual use of the “molecule-frame” (MF) convention. He states that the MF convention, of assigning unhindered “concentrated-gas” entropies to solutes, is the approach taken by theories based on continuum-solvation models. Since continuum-solvation models appear to be aiming to produce solvation Gibbs energies directly, and no distinction between ΔH_{solv} and ΔG_{solv} is made, problems in estimating either ΔH_{solv} or ΔG_{solv} may occur. Hence, when we first tested “concentrated-gas” entropies in the MF convention and began to see inaccuracies when comparing to experimental results, we switched to an SF convention and desired a damping method. There is a “one-factor-fits-all” entropy-damping method published by Wertz in 1980:³⁶

$$\delta_{\text{damp}}S = \Delta S_{\text{solvation}} = -0.46(S^\circ_{\text{gas}} - 14.3)$$

but, as he noted, certain classes of molecules revealed systematic errors (for instance, the method damped too much for molecules with nearly free internal rotation). We developed a more sophisticated method for more accuracy.

To calibrate a new entropy damping method, we wanted a method that, in the limit of mole fraction = 1, would reproduce the condensation thermochemistry of “Trouton” solvents, i.e. solvents whose $\Delta S_{\text{vaporization}}$ is roughly 21 eu (cal mol^{−1} K^{−1}) at their boiling points.^{37,38} For Trouton solvents, which include THF, hexane, diethyl ether, benzene, neopentane, dichloromethane, and acetone, a perusal of standard enthalpies of formation and standard entropies at 298 K (i.e., not at boiling points) gives values for ΔH_{cond} , $T\Delta S_{\text{cond}}$, and ΔG_{cond} of −8, −7, and −1 kcal mol^{−1} (which puts ΔS_{cond} (298K) at −23 eu instead of −21 eu). Attempts to reproduce these values with current continuum-solvation models will poorly predict the ΔH value, the ΔG value, or both, due to ignoring or mistreating the damping of entropy that is inherent in forcing molecules into condensed phases.

The entropy-damping terms introduced below, when applied to $T\Delta S_{\text{cond}}$ for THF, reproduced the correct −7 kcal mol^{−1} value. We went on to try to reproduce ΔH_{cond} and/or ΔG_{cond} for THF using the PCM model in Gaussian09, but obtained energy values of −2, −12, +4, and −4, depending on whether we included terms II, II + III, II + III + IV, or “SMD” II + III + IV (using the alternative PCM parameters from SCRF = SMD^{14,39}). None of these compare well to the value of −8 for ΔH_{cond} . The first and last values agree well with the value of −1 for ΔG_{cond} but arise from different decisions regarding terms III and IV (should these be in a condensation calculation?). This disagreement, combined with our past concerns with the sensitivity of $\delta_{\text{disp}}E$ (III) and $\delta_{\text{cav}}E$ (IV) to cavity size in the PCM model,⁴⁰ and the belief that terms III and IV are less important in $\Delta_{\text{rxn}}G$ than for ΔG_{cond} or $\Delta G_{\text{solvation}}$, led us to abandon these terms in the current project. (We did test $\delta_{\text{disp}}E$ and $\delta_{\text{cav}}E$ effects but only for the dissociation of the adduct 9BBN·THF, and found reasonable cancellation: $\Delta_{\text{rxn}}E$ was 12.4 with only II, 13.4 with II + III + IV, and 12.8 with “SMD” II + III + IV.)

The four solvation terms used were as follows:

Solvation II—Polarization of E_{elec} . Add $E[\text{PCM/B3LYP/6-31G(d)}/\text{B3LYP/6-31G(d)}] - E[\text{B3LYP/6-31G(d)}]$ for each compound, using the Gaussian09 polarizable-continuum model (PCM, keyword SCRF=(solvent=thf)),^{32,33} which by default in Gaussian09 includes $\delta_{\text{polz}}E$ but neither $\delta_{\text{disp}}E$ nor $\delta_{\text{cav}}E$.

Solvation VII—Damping of PV . Subtract $RT = 0.592$ kcal mol^{−1} for each compound. This removes the $PV = RT$ term added in $G_{\text{gas,init}}$. In solution, PV should be closer to zero than to its gas-phase value.

Solvation VIII—Damping of TS_{trans} . Add three terms:

$$\delta_{\text{damp}} TS_{\text{trans}} = T(\Delta S_{\text{solvent}} + \Delta S_{\text{comp}} + \Delta S_{\text{hind}})$$

$$\Delta S_{\text{solvent}} = \left(\frac{c_{\text{liq}} - c}{c} \right) R \ln \left(\frac{c^{-1}}{c^{-1} - c_{\text{liq}}^{-1}} \right) \quad (\text{solvent expansion})$$

$$\Delta S_{\text{comp}} = R \ln \left(\frac{c^{-1}}{\bar{V}_{\text{gas}}^{\circ}} \right) \quad (\text{solute compression})$$

$$\Delta S_{\text{hind}} = R \ln \left(\frac{\bar{V}_{\text{eff}}}{c_{\text{liq}}^{-1}} \right) \quad (\text{solute hindrance})$$

where c is the desired concentration of solute (here 1 M), c_{liq} is the concentration of pure solvent (here 12.3 M for THF), $\bar{V}_{\text{gas}}^{\circ}$ is the standard molar volume of an ideal gas (24.466 L mol⁻¹ at 298.15 K and 1 atm), and \bar{V}_{eff} is an effective molar free volume of $(1.5 \text{ \AA})^3 N_{\text{AVO}} = 0.002032 \text{ L}$ per mole of solute molecules. This formula comes from the following arguments.

All three terms were derived from the basic concentration-change formula $nR \ln(V_f/V_i)$. The first comes from expanding the solvent to make room for incoming solute, a term commonly ignored. Per mole of solute dissolved, this is an expansion of $(c_{\text{liq}} - c)/c$ moles of solvent; for expansion of THF for 1 M solutes we expand $(c_{\text{liq}} - c)/c = 11.3 \text{ mol THF}$ from $V_i = 0.919 \text{ L}$ to $V_f = 1 \text{ L}$, obtaining $\Delta S_{\text{solvent}} = +1.90 \text{ eu}$ (cal mol⁻¹ K⁻¹). The second term ΔS_{comp} is the compression of 1 mol gaseous solute from standard gas volume $V_i = 24.466 \text{ L}$ to the volume appropriate for the desired solution concentration (here $V_f = 1 \text{ L}$), and hence $\Delta S_{\text{comp}} = -6.35 \text{ eu}$. Note that this value gives rise to $T\Delta S_{\text{comp}} = -1.9 \text{ kcal mol}^{-1}$, the common standard-state shift applied to G_{gas} before considering the act of solvation under the constant- ρ convention described by Ben-Naim.⁴¹

The third term ΔS_{hind} is the damping term due to translations being hindered in the liquid state due to the presence of other molecules. We suppose that a solute-molecule translation hindrance is roughly equal to a solvent-molecule translation hindrance when conceptually changing from “concentrated gas” (a gas at solvent concentration c_{liq}) to pure liquid. Hence we consider 1 mol of solvent, use $V_i = c_{\text{liq}}^{-1}$ (i.e., each molecule freely translates in the molar volume, which for THF is 0.081 L), and for V_f we restrict each molecule to a solvent cage allowing rattling motions equivalent to a collapsed-point solute molecule undergoing free translation in a $(1.5 \text{ \AA})^3$ volume. Support for this idea comes from Ewing, who in the 1960s noted that quantized translational energy spacings of $\sim 100 \text{ cm}^{-1}$ were determined from the band envelope of rotational spectral bands from a solution of H_2 in liquid Ar, and further pointed out that a particle-in-a-box model with a box width of $\sim 1 \text{ \AA}$ reproduces this spacing.⁴² Since the solutes here have atoms of wider electron distributions than H_2 , we increased the box width to an arbitrary value of 1.5 Å. Hence, $V_f = \bar{V}_{\text{eff}} = (1.5 \text{ \AA})^3 N_{\text{AVO}} = 0.002032 \text{ L}$, producing $\Delta S_{\text{hind}} = -7.33 \text{ eu}$. While ΔS_{hind} is independent of solute concentration, $\Delta S_{\text{solvent}}$ and ΔS_{comp} are not. Note that Henschman treats this damping with a more laborious procedure, by assuming harmonic oscillations (rather than free translations) in the solvent cage, and running dynamics simulations to obtain the relevant force constants.³⁵

The sum of the three corrections for 1 M solute in THF is $\delta_{\text{damp}} S_{\text{trans}} = -11.8 \text{ eu}$. Note that in the limit as $c \rightarrow c_{\text{liq}}$, our $\delta_{\text{damp}} S_{\text{trans}}$ method extrapolates properly to the case of the solute becoming a pure liquid of concentration c_{liq} , and thus can be used to compare to Trouton’s rule. Considering THF as the solute, and removing arbitrary solvent by extrapolating $c \rightarrow c_{\text{liq}}$, the three terms $\Delta S_{\text{solvent}} + \Delta S_{\text{comp}} + \Delta S_{\text{hind}}$ extrapolate to $0 - 11.3 - 7.3 = -18.6 \text{ eu}$. With further damping of S_{rot} (below) of $\sim 4 \text{ eu}$, we achieve the Trouton 298 K value of -23 eu .

Solvation IX—Damping of TS_{rot} . Writing S_{rot} as a sum of three principal-axis components (S_a, S_b, S_c), add a damping correction for each component, as follows:

$$\delta_{\text{damp}} TS_{\text{rot}} = T(\delta S_a + \delta S_b + \delta S_c)$$

$$\delta S_i = -d_i S_i^{\text{gas}}$$

$$d_i = 0.3 + (0.4/\pi) \tan^{-1}[2S(t_i - 0.5)]$$

$$t_a = \frac{(L_b - L_c)L_b L_c}{\langle L_{\text{solvent}} \rangle^3}, \quad t_b = \frac{(L_a - L_c)L_a L_c}{\langle L_{\text{solvent}} \rangle^3},$$

$$t_c = \frac{(L_a - L_b)L_a L_b}{\langle L_{\text{solvent}} \rangle^3}$$

$$L_a = \sqrt{\frac{8(I_b + I_c - I_a)}{M}}, \quad L_b = \sqrt{\frac{8(I_a + I_c - I_b)}{M}},$$

$$L_c = \sqrt{\frac{8(I_a + I_b - I_c)}{M}}$$

We refer to d_i as the *rotational entropy damping term*, a value between 0.1 (minimal damping of rotation) and 0.5 (strong damping). It depends on a dimensionless *tumbling parameter* t_i , which itself depends on the lengths of the solute molecule along each principal axis (L_a, L_b, L_c) and the average of the same three lengths of the solvent molecule, $\langle L_{\text{solvent}} \rangle$. These lengths are obtained in a crude approximation from the mass M and moments of inertia (I_a, I_b, I_c) of the molecule. Thus, the d_i terms require only the M and I_i which are commonly output in quantum chemistry programs.

The tumbling parameter t_i was designed so that $t_i > 0.5$ would denote tumbling that would be significantly hindered in solution; large t_i would result from large $L_{\text{solute}}/L_{\text{solvent}}$ ratios, and large $L_b - L_c$ differences (i.e., spherical solutes regardless of size would have $t_i = 0$ and be minimally hindered). The \tan^{-1} function in d_i was chosen for an intuitively sudden but smooth transition from minimally hindered rotation to a seesaw-like wobbling vibration as t_i crosses 0.5 (Figure 2).

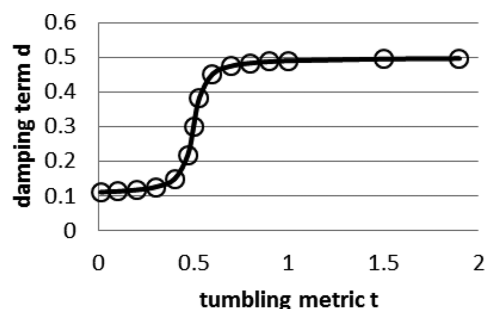


Figure 2. Plot of the rotational entropy damping term d as a function of tumbling metric t .

The square-root formulas for the effective molecule lengths L_i arise as follows. Assume that the mass distribution about a given axis (say, z -axis) is a uniform solid ellipse bound by the curve $(y/y_0)^2 + (x/x_0)^2 = 1$, i.e., $y_{\text{bound}} = y_0[1 - (x/x_0)^2]^{1/2}$, where $y_0 = L_y/2$ and $x_0 = L_x/2$. Then, if r is the radial distance of a point of mass from the z axis,

$$\begin{aligned}\langle r^2 \rangle &= \frac{\int_{x=0}^{x_0} \int_{y=0}^{y_{\text{bound}}} r^2 \, dy dx}{\int_{x=0}^{x_0} \int_{y=0}^{y_{\text{bound}}} dy dx} \\ &= \frac{(\pi/16)(y_0^3 x_0^3 + y_0^3 x_0)}{(\pi/4)(y_0 x_0)} \\ &= \frac{1}{4}(x_0^2 + y_0^2) \\ &= \frac{1}{16}(L_x^2 + L_y^2)\end{aligned}$$

This expression can be substituted into

$$I_z = \sum_{i=1}^{\text{atoms}} m_i r_i^2 \approx M \langle r^2 \rangle = \frac{M}{16}(L_x^2 + L_y^2)$$

from which the square-root expressions for the lengths L_i follow.

As a last detail, the gas-phase rotational entropy S_{rot} was divided into components S_a , S_b , and S_c according to

$$\frac{S_a}{Nk} = \frac{1}{2} + \ln \left(\left[\frac{8\pi^2 I_a kT}{h^2} \right]^{1/2} \frac{\pi^{1/6}}{\sigma^{1/3}} \right)$$

where σ is the overall rotational symmetry number.

Computed data for this solvation IX correction appear in Supporting Information, and were based on B3LYP/6-31G(d) molecular geometries.

The Concentrated-Gas (cg) Approximation. We will compare the results of our method to results obtained with a more common procedure that we term a “concentrated-gas” or cg method. In this method, the damping terms VII–IX (Table 1) are ignored except for the gas-compression term ΔS_{comp} of term VIII.

3. RESULTS AND DISCUSSION

Spectral Signatures. The ^{11}B -NMR spectrum was used by Wang and Brown² to identify the presence of the 9BBN·THF adduct. They attributed observed signals to the (9BBN)₂ dimer ($\delta_{\text{rel}} = 28$) and 9BBN·THF complex ($\delta_{\text{rel}} = 14$). Our results confirm this assignment (Table 2). A peak due to 9BBN monomer would be much further shifted ($\delta_{\text{rel}} = 90$ –95).

Table 2. ^{11}B -NMR Chemical Shifts, GIAO B3LYP/6-311+G(d,p)//B3LYP/6-31G(d)

species	DFT δ absolute	DFT δ relative ^b	expt ^a δ relative ^b
BF ₃ ·OEt ₂	101.5	0.0	0.0
9BBN·THF	83.9	17.6	13.8
(9BBN) ₂	75.3	26.2	27.7
9BBN	8.5	93.0	n/a

^aWang and Brown.² ^bRelative to BF₃·OEt₂.

Infrared spectra were also used by Wang and Brown² to identify the presence of the 9BBN·THF adduct. In the B–H stretch region, they attributed a small peak at 2300 cm^{−1} to be

Table 3. Signature BH Stretch Infrared Mode, B3LYP/6-31G(d)

species	DFT ω , cm ^{−1}	DFT ^a ν , cm ^{−1}	expt ^b ν , cm ^{−1}
9BBN	2617	2516	n/a
THF·9BBN	2445	2350	2300
(9BBN) ₂	1678	1613	1570

^aUsing 0.9613 scale factor.²⁷ ^bWang and Brown.²

due to the adduct, and a strong peak at 1570 cm^{−1} to be due to BH bridge bonds of the (9BBN)₂ dimer. Our results confirm this also (Table 3): by converting our computed harmonic frequencies ω to fundamentals ν using a recommended scaling factor²⁷ of 0.9613, we obtain computed values only 2% larger than the experimental values (a scaling factor of 0.94 would have been ideal). The corresponding absorption for a monomer would be near 2460–2520 cm^{−1}, which was apparently not observed. The relevant B3LYP/6-31G(d) predicted spectra appear in the Supporting Information (Figure S1). The intense peak of the dimer is due to the normal mode involving the bridging hydrogens moving parallel to the B–B axis.

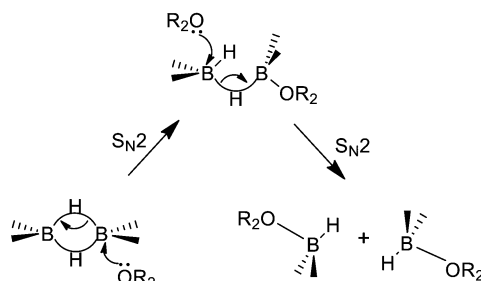
Mechanism of Solvolysis Stage. Ignored to date has been the possibility that THF solvolysis of borane dimers might feature an intermediate in which one of the two BHB hydride bridges remains in place. We have computationally found such intermediates for both B₂H₆ and (9BBN)₂ (Supporting Information, Figure S2). Hence, the mechanism possibilities for overall solvolysis reaction R1 could be S_N2 + S_N2 (R2 + R3), S_N2 + S_N1 (R2 + R5 + R6), or S_N1 + S_N1 (R4 + R6 + R6) (Scheme 1).

First, we wish to point out large errors in B3LYP binding energies when using the secondary borane 9BBN: binding energies for reactions R4, R5, and −R6 are all underestimated by 9–13 kcal mol^{−1} relative to CCSD(T) results (Table 4). No such problem exists when using BH₃ (Table 5). Some side tests on methylboranes indicate that the problems might be general with secondary boranes, which have a more electropositive boron atom than BH₃. We tried two other double- ζ basis sets with no improvement (very little effect, at most 1.4 kcal mol^{−1}). We tried two other DFTs, but OLYP was much worse (errors of >15 kcal mol^{−1} for the overall reaction R1, due to poor adduct binding energies), and PBE was inconsistent (a poor reaction R4 binding energy for BH₃ dimer but not 9BBN dimer).

Second, the computed Gibbs energy profiles for the solvolysis stage are plotted in Figure 3 for both B₂H₆ and (9BBN)₂; they include the three S_N2 transition states found. Values of ΔH and ΔG for each step, including ΔG with the cg approximation, are tabulated in the Supporting Information. There are large differences in profile between the two diboranes. For B₂H₆ the mechanism is S_N2 + S_N1, i.e. S_N2 conversion to the SBB intermediate, followed by S_N1 rupture of the remaining H-bridge bond. For (9BBN)₂ the mechanism might appear to be S_N1 + S_N1, which would disagree with Brown, but the S_N2 barrier for step R2 is within 3 kcal mol^{−1} of the S_N1 in this figure, and a closer inspection of minor effects is warranted. We first perform four comparisons with experimental data to support the accuracy of the results.

Comparison 1: K for Reaction R1, $B = \text{BH}_3$. Solutions of B₂H₆ in THF are known to be dominated by the adduct BH₃·THF and not B₂H₆.³ Figure 3 appears to show that adduct formation is not favored ($\Delta_{\text{rxn}}G^\circ = +1.1$ kcal mol^{−1}), but this simple check is incorrect, due to concentration and $\Delta_{\text{rxn}}n$ effects. One first must take this standard (1 M) result, convert

Scheme 1. Overall Solvolysis Reaction (R1), Its Possible Elementary Steps (R2–R6), and Depiction of the R2 + R3 Hypothesis for Reaction R1^a



^aS = OR₂ (solvent), B = BR₂H (borane).

it to an equilibrium constant ($K^\circ = e^{-\Delta G^\circ/RT} = 0.2$), invoke its expression as a ratio of molarity products:

$$\begin{aligned}
 K &= \frac{[\text{BS}]^2}{[\text{B}_2][\text{S}]^2} = 0.2 \text{ M}^{-1} \\
 \Rightarrow \frac{[\text{BS}]^2}{[\text{B}_2]} &= K[\text{S}]^2 \approx (0.2 \text{ M}^{-1})(12.3 \text{ M})^2 = 30 \text{ M}
 \end{aligned}$$

and realize that this produces $[\text{BS}] \gg [\text{B}_2]$ at typical concentrations, for instance if $[\text{BS}] = 0.3 \text{ M}$ then $[\text{B}_2] = 0.003 \text{ M}$. The cg approximation in our hands (see Methods) gives $\Delta_{\text{rxn}}G^\circ = -0.2 \text{ kcal mol}^{-1}$, which also results in $[\text{BS}] \gg [\text{B}_2]$.

Comparison 2: ΔG° for Reaction R1, B = 9BBN. For this Brown² derived an equilibrium constant value of $8.05 \times 10^{-5} \text{ M}^{-1}$, corresponding to $\Delta_{\text{rxn}}G^\circ = +5.6 \text{ kcal mol}^{-1}$ (his eq 11). Our method obtains $+5.0 \text{ kcal mol}^{-1}$ (in THF; our gas-phase result is $+9.7$). The cg value in our hands gives $+4.9 \text{ kcal mol}^{-1}$, also in very good agreement with experiment.

Comparison 3: $\Delta^\ddagger G^\circ$ for Reaction R4, B = 9BBN. Brown² reported rate constants of $k_1 = 1.5 \times 10^{-4} \text{ s}^{-1}$ for dimer loss ($d[\text{B}_2]/dt = -k_1[\text{B}_2]$) when performing (9BBN)₂ hydroborations

Table 4. Results for ΔE_{elec} for Reactions R1–R6 for 9BBN Dimer

reaction	OLYP/6-31G(d)	PBEPBE/6-31G(d)	B3LYP/6-31G(d)	B3LYP/6-31G(d,p)	B3LYP/cc-pVDZ	CCSD(T)/cc-pVDZ ^a
R1: B ₂ + 2S → 2SB	17.2	3.9	1.1	2.0	1.4	−8.5
R2: B ₂ + S → SBB	DNE ^b	9.1	9.0	9.8	10.1	−0.3
R3: SBB + S → 2SB	DNE	−5.2	−7.9	−7.8	−8.7	−8.2
R4: B ₂ → 2B	23.1	34.3	23.5	24.5	24.9	36.7
R5: SBB → SB + B	DNE	10.0	3.3	3.4	3.1	14.4
R6: B + S → SB	−2.9	−15.2	−11.2	−11.3	−11.7	−22.6

^aSingle-point calculations at B3LYP/6-31G(d) geometries. ^bDNE: does not exist.

Table 5. Results for ΔE_{elec} (kcal mol^{−1}) for Reactions R1–R6 for B₂H₆

reaction	OLYP/6-31G(d)	PBEPBE/6-31G(d)	B3LYP/6-31G(d)	B3LYP/6-31G(d,p)	B3LYP/cc-pVDZ	CCSD(T)/cc-pVDZ ^a
R1: B ₂ + 2S → 2SB	9.2	−0.4	−3.4	−2.2	−3.6	−8.3
R2: B ₂ + S → SBB	11.5	1.8	1.5	2.2	1.8	−1.1
R3: SBB + S → 2SB	−2.3	−2.3	−4.9	−4.4	−5.3	−7.2
R4: B ₂ → 2B	41.8	51.0	39.1	40.2	39.5	39.4
R5: SBB → SB + B	14.0	23.5	16.3	16.8	16.2	16.7
R6: B + S → SB	−16.3	−25.7	−21.2	−21.2	−21.5	−23.9

^aSingle-point calculations at B3LYP/6-31G(d) geometries.

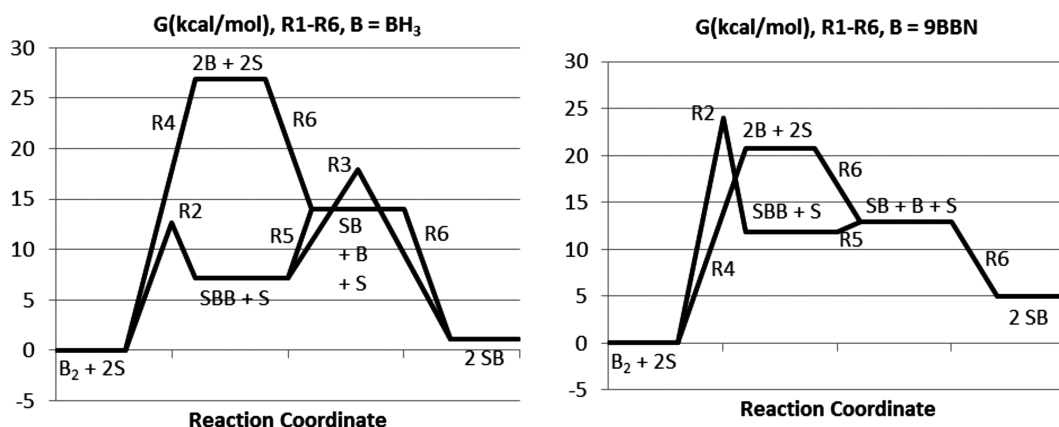


Figure 3. Gibbs energy profiles of the solvolysis reaction R1 and its elementary reactions R2–R6, from our composite method applied to THF solutions (298 K, 1 mol L^{−1}).

of “fast” alkenes in noncomplexing nonpolar solvents like CCl_4 or cyclohexane (his Table 1). From the Eyring equation (Appendix B) one derives $\Delta^\ddagger G^\circ(\text{expt}) = 22.7 \text{ kcal mol}^{-1}$. Taking our computed value for $\Delta_{\text{rxn}} G^\circ$ for $(9\text{BBN})_2$ dissociation in THF (20.8), removing the THF polarization effect (adding 0.4), and adding a vTST $\delta_{\text{FES}} G$ correction (1.8, see Methods), we obtain $\Delta^\ddagger G^\circ = 23.0 \text{ kcal mol}^{-1}$. The cg method produces $18.8 \text{ kcal mol}^{-1}$, which is outside our goal of 2 kcal mol^{-1} accuracy.

Comparison 4: $\Delta^\ddagger G^\circ$ for Reaction R2 in THF, $B = 9\text{BBN}$. Brown² reported a $10\times$ faster rate of dimer loss ($k_1^{\text{eff}} = 1.42 \times 10^{-3} \text{ s}^{-1}$) when performing $(9\text{BBN})_2$ hydroborations of “fast” alkenes in THF, instead of in noncomplexing nonpolar solvents (his Table 1). He proposed that this is due to a solvolysis stage in THF, the rate being governed by an $\text{S}_{\text{N}}2$ step, $\text{R2}(B = 9\text{BBN})$. Note that solvolysis of $(9\text{BBN})_2$ involves only one $\text{S}_{\text{N}}2$ step (Figure 3, right), unlike that of B_2H_6 which requires two (Figure 3, left). In an $\text{S}_{\text{N}}2$ step, the rate of dimer loss is $d[\text{B}_2]/dt = -k_2[\text{S}][\text{B}_2] = -k_1^{\text{eff}}[\text{B}_2]$, so $k_2 = k_1^{\text{eff}}/[\text{S}] = 1.15 \times 10^{-4} \text{ M}^{-1} \text{ s}^{-1}$ which by Eyring gives $\Delta^\ddagger G^\circ(\text{expt}) = 22.8 \text{ kcal mol}^{-1}$. Our method (using the optimized $\text{S}_{\text{N}}2$ transition-state geometry, i.e. straight from Figure 3) gives 24.0, while the cg method gives 24.6. Again our method appears to improve upon the cg method.

Application 1: $\text{S}_{\text{N}}1$ vs $\text{S}_{\text{N}}2$ Rate for Reaction R1 in THF, $B = 9\text{BBN}$. Since Figure 3 (right) shows that the reaction R2 $\text{S}_{\text{N}}2$ Gibbs barrier is only 3 kcal mol^{-1} higher than the reaction R4 $\text{S}_{\text{N}}1$ dissociation Gibbs energy, it is better to focus on the rate law ratio $v(\text{S}_{\text{N}}2)/v(\text{S}_{\text{N}}1)$, where other factors that need be considered are (i) rate law complexity, (ii) $[\text{THF}]$ effects, and (iii) a vTST correction for $\Delta^\ddagger G^\circ(\text{S}_{\text{N}}1)$.

We start with factor i. While the rate law for $\text{S}_{\text{N}}2$ step dimer loss in $(9\text{BBN})_2$ solvolysis is elementary, the general $\text{S}_{\text{N}}1$ steady-state rate expression (from reactions R4, R-4, and R6) is⁴³

$$\frac{d[\text{B}_2]}{dt} = \frac{-\frac{1}{2}k_4k_6[\text{B}_2][\text{S}]}{k_{-4}[\text{B}] + \frac{1}{2}k_6[\text{S}]}$$

but for “fast” alkenes $k_{-4}[\text{B}] \ll (1/2)k_6[\text{S}]$, so the rate law collapses to

$$\frac{d[\text{B}_2]}{dt} = -k_4[\text{B}_2]$$

which is an elementary step. This k_4 is the k_1 of Brown,² just as it was for noncomplexing solvents (comparison 3). Since the $\text{S}_{\text{N}}2$ rate law was $d[\text{B}_2]/dt = -k_2[\text{S}][\text{B}_2] = -k_1^{\text{eff}}[\text{B}_2]$ (comparison 4), the rate ratio is

$$\frac{v_{\text{S}_{\text{N}}2}}{v_{\text{S}_{\text{N}}1}} = \frac{\frac{d[\text{B}_2]}{dt}(\text{S}_{\text{N}}2)}{\frac{d[\text{B}_2]}{dt}(\text{S}_{\text{N}}1)} = \frac{k_1^{\text{eff}}(\text{S}_{\text{N}}2)}{k_1(\text{S}_{\text{N}}1)} = \frac{k_2(\text{S}_{\text{N}}2)[\text{S}]}{k_4(\text{S}_{\text{N}}1)}$$

where we see effect ii: the $\text{S}_{\text{N}}2$ rate depends on THF concentration $[\text{S}]$. Effect iii, the vTST correction, is used inside $k_1(\text{S}_{\text{N}}1)$ to convert $\Delta G^\circ(\text{B}_2 \rightarrow 2\text{B})$ to $\Delta^\ddagger G^\circ$. With the vTST and $[\text{THF}]$ effects incorporated, the predicted rate ratio is 1.1, indicating that the $\text{S}_{\text{N}}2$ pathway leads to a faster rate (in agreement with Brown, and the reverse of the conclusion from the naïve curve comparison in Figure 3). The cg method produces a rate ratio of 0.0013, which erroneously predicts an $\text{S}_{\text{N}}1$ pathway for $9\text{BBN} \cdot \text{THF}$ adduct formation. The correct prediction from our method is somewhat fortuitous, as we are expecting an accuracy of only a factor of 30 in a rate constant (see Appendix B); however, this is a vast improvement from the

cg result, whose rate ratio must be in error by three orders of magnitude.

We can also use the above results to predict the catalytic speedup of using THF as solvent. This would be the rate ratio $k_1^{\text{eff}}(\text{S}_{\text{N}}2, \text{THF})/k_1(\text{S}_{\text{N}}1, \text{CCl}_4)$, which from Brown's data² is $0.00142/0.00015 = 9.5$. Using our $\Delta^\ddagger G^\circ$ values, our method gives a rate ratio of 2.3, while the cg method gives 0.0027. The cg method predicts no catalytic speedup; our method is again fortuitous with its correct qualitative prediction.

Our first conclusion is that one should not venture to make a conclusion regarding $\text{S}_{\text{N}}1$ vs $\text{S}_{\text{N}}2$ mechanisms if our method gives their ab initio rates to be within a factor of 30. Our second conclusion is that the cg method is likely to be *less reliable* than ours for such rate comparisons.

Mechanism of the Alkene-Addition Stage. We pursued this step only as far as the monoalkylborane $\text{Me}_2\text{CHCH}_2\text{BR}_2$, since ensuing exothermic steps (complexation to solvent or addition of another alkene) would then be straightforward extensions. Given the (computationally) known π -complex intermediate $\text{BH}_3 \cdot \text{alkene}$, which undergoes a fast 4-electron rearrangement to the monoalkylborane, the mechanism possibilities for overall alkene-addition reaction R7 are then $\text{S}_{\text{N}}2 + 4\text{e}$ (reactions R8 + R11), or $\text{S}_{\text{N}}1 + 4\text{e}$ (reactions R9 + R10 + R11) (Scheme 2).

For reaction energetics, again B3LYP performed poorly for $B = 9\text{BBN}$ but well for $B = \text{BH}_3$ (Tables 6 and 7), due again to the poorly predicted $9\text{BBN} \cdot \text{THF}$ binding energy. OLYP and PBE are rated worse because they do not produce the $\text{BH}_3 \cdot \text{C}_4\text{H}_8$ π -complex.

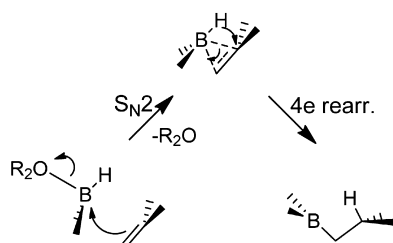
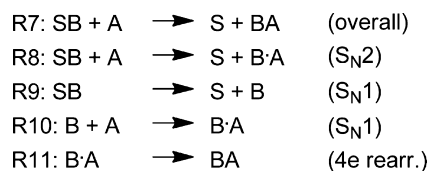
Second, the computed Gibbs energy profiles for this alkene-addition stage are plotted in Figure 4 for both B_2H_6 and $(9\text{BBN})_2$; they include the three $\text{S}_{\text{N}}2$ transition states found. Values of ΔH and ΔG for each step, including $\Delta G(\text{cg})$, are tabulated in the Supporting Information. For $(9\text{BBN})_2$ (right plot) the mechanism is $\text{S}_{\text{N}}1 + 4\text{e}$, i.e. $\text{S}_{\text{N}}1$ dissociation of the adducts, followed by 4e rearrangement without any $9\text{BBN} \cdot \text{C}_4\text{H}_8$ π -complex involved. For B_2H_6 the mechanism might appear to be $\text{S}_{\text{N}}1 + 4\text{e}$, but the $\text{S}_{\text{N}}2$ barrier for step R8 is within 3 kcal mol^{-1} of the $\text{S}_{\text{N}}1$ in this figure, and hence a closer inspection of minor effects is warranted once again.

Application 2: $\text{S}_{\text{N}}1$ vs $\text{S}_{\text{N}}2$ Rate for Reaction R7 in THF, $B = \text{BH}_3$. Again as in application 1 it is better to focus on the rate law ratio $v(\text{S}_{\text{N}}2)/v(\text{S}_{\text{N}}1)$ than a simple free energy comparison, and consider (i) rate law complexity, (ii) $[\text{THF}]$ effects, and (iii) a vTST correction for $\Delta^\ddagger G^\circ(\text{S}_{\text{N}}1)$. Although Singleton did factor in effects ii and iii in his recent comparison,¹¹ he used the less reliable cg method (and it is not clear to us how the THF concentration was used).

Pasto³ reported a rate constant of $k_2 = 1.6 \text{ M}^{-1} \text{ s}^{-1}$ for alkylborane production ($d[\text{BA}]/dt = k_2[\text{SB}][\text{A}]$) when performing hydroboration of tetramethylethylene with $\text{BH}_3 \cdot \text{THF}$ adducts in THF at 25°C (his Table 1). He thought the mechanism was $\text{S}_{\text{N}}2$ (reaction R8; at that time the ensuing instantaneous reaction R11 step was not known), from second order kinetics. However, Brown⁵ demonstrated that second order kinetics for product formation can also be achieved by an $\text{S}_{\text{N}}1$ mechanism (with monomeric borane as intermediate) as long as the rate for the $\text{B} + \text{S}$ back-reaction (reaction R-9) was faster than the $\text{B} + \text{A}$ step (reaction R10), because the $\text{S}_{\text{N}}1$ steady-state rate law for product formation is⁵

$$\frac{d[\text{BA}]}{dt} = \frac{k_9k_{10}[\text{BS}][\text{A}]}{k_{-9}[\text{S}] + k_{10}[\text{A}]}$$

Scheme 2. Overall Alkene-Addition Reaction (R7), Its Possible Elementary Steps (R8–R11), and Depiction of the R8 + R11 Hypothesis for Reaction R7^a



^aS = OR₂ (solvent), B = BR₂H (borane), A = C_nH_{2n} (alkene).

which can be written

$$\frac{d[\text{BA}]}{dt} = k_2^{\text{eff}}[\text{BS}][\text{A}], \quad k_2^{\text{eff}} = \frac{k_9 k_{10}}{k_{-9}[\text{S}] + k_{10}[\text{A}]} \approx \frac{k_9 k_{10}}{k_{-9}[\text{S}]}$$

if $k_{-9}[\text{S}] \gg k_{10}[\text{A}]$. The rate law ratio $v(\text{S}_{\text{N}2})/v(\text{S}_{\text{N}1})$ in this case becomes

$$\begin{aligned} \frac{v_{\text{S}_{\text{N}2}}}{v_{\text{S}_{\text{N}1}}} &= \frac{\frac{d[\text{BA}]}{dt}(\text{S}_{\text{N}2})}{\frac{d[\text{BA}]}{dt}(\text{S}_{\text{N}1})} \\ &= \frac{k_2(\text{S}_{\text{N}2})}{k_2^{\text{eff}}(\text{S}_{\text{N}1})} \approx \frac{k_8(\text{S}_{\text{N}2})k_{-9}[\text{S}]}{k_9(\text{S}_{\text{N}1})k_{10}} \approx \frac{k_8(\text{S}_{\text{N}2})[\text{S}]}{k_9(\text{S}_{\text{N}1})} \end{aligned}$$

but note that we compute the full k_2^{eff} for the ratio and do not make the approximations indicated.

Brown further went on to prove that the S_N1 mechanism for BH₃ adducts was operating in some non-THF systems in which [S] was neither THF nor solvent, but alternative complexing Lewis bases (Me₂S, Et₃N) at solute concentrations (<1 M) in toluene solvent.⁵ Thus, in Brown's cases, it must be true that $k_2^{\text{eff}}(\text{S}_{\text{N}1}) > k_2(\text{S}_{\text{N}2})$. However, there may be lingering doubt about the mechanism in THF solvent, because (a) ethers may have different binding energies than amines or sulfides, and (b) in THF [S] \approx 12.3 M, which reduces k_2^{eff} (and thus the S_N1 rate) by a factor of 12.3.

From our $\Delta^\ddagger G^\circ$ value for the S_N2 path (reaction R8(TS), 16.5 kcal mol⁻¹), the Eyring equation gives $k_2(\text{S}_{\text{N}2}) = 4.6 \text{ M}^{-1} \text{ s}^{-1}$, in close agreement with $k_2(\text{expt}) = 1.6$. However, we compute $k_2^{\text{eff}}(\text{S}_{\text{N}1}) = 8.0 \text{ M}^{-1} \text{ s}^{-1}$, which is faster. Hence our predicted rate ratio is $v(\text{S}_{\text{N}2})/v(\text{S}_{\text{N}1}) \approx 0.6$, i.e. for every

Table 6. Results for ΔE_{elec} (kcal mol⁻¹) for Reactions R7–R11 for 9BBN Dimer

reaction	OLYP/6-31G(d)	PBEPBE/6-31G(d)	B3LYP/6-31G(d)	B3LYP/6-31G(d,p)	B3LYP/cc-pVDZ	CCSD(T)/cc-pVDZ ^a
R7: SB + A \rightarrow S + BA	-59.3	-16.2	-15.6	-16.1	-15.2	-11.2
R8: SB + A \rightarrow S + B·A	DNE ^b	DNE	DNE	DNE	DNE	DNE
R9: SB \rightarrow S + B	2.9	15.2	11.2	11.3	11.7	22.6
R10: B + A \rightarrow B·A	DNE	DNE	DNE	DNE	DNE	DNE
R11: B·A \rightarrow BA	DNE	DNE	DNE	DNE	DNE	DNE

^aSingle-point calculations at B3LYP/6-31G(d) geometries. ^bDNE: does not exist.

Table 7. Results for ΔE_{elec} (kcal mol⁻¹) for Reactions R7–R11 for B₂H₆

reaction	OLYP/6-31G(d)	PBEPBE/6-31G(d)	B3LYP/6-31G(d)	B3LYP/6-31G(d,p)	B3LYP/cc-pVDZ	CCSD(T)/cc-pVDZ ^a
R7: SB + A \rightarrow S + BA	-10.2	-7.8	-7.6	-8.2	-7.8	-7.5
R8: SB + A \rightarrow S + B·A	DNE ^b	DNE	9.8	9.6	10.0	11.3
R9: SB \rightarrow S + B	16.3	25.7	21.2	21.2	21.5	23.9
R10: B + A \rightarrow B·A	DNE	DNE	-11.4	-11.6	-11.5	-12.6
R11: B·A \rightarrow BA	DNE	DNE	-17.5	-17.8	-17.8	-18.8

^aSingle-point calculations at B3LYP/6-31G(d) geometries. ^bDNE: does not exist.

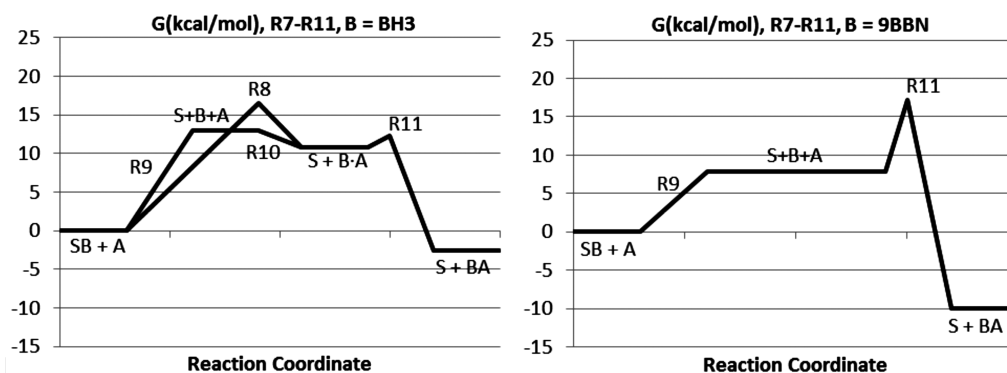


Figure 4. Gibbs energy profiles of the alkene-addition reaction R7 and its elementary reactions R8–R11, from our composite method applied to THF solutions (298 K, 1 mol L⁻¹). In the right-hand plot, reaction R11 (4e⁻ rearrangement) starts from fully dissociated reactants because the π -complex 9BBN·C₄H₈ does not exist.

8 product molecules, 3 came from an S_N2 mechanism. This predicted S_N1 dominance agrees with Brown and not Pasto, but the results are within an order of magnitude, which cannot be considered conclusive since our accuracy is worse than that. (The less accurate cg approximation in our hands gave $k_2(S_N2) = 0.33 \text{ M}^{-1} \text{ s}^{-1}$, $k_2^{\text{eff}}(S_N1) = 4.3 \text{ M}^{-1} \text{ s}^{-1}$, and hence a rate ratio of 0.077, which from application 1 we know to be an equally inconclusive result.)

Comparison 5: E_a for Reaction R7 in THF, $B = \text{BH}_3$. We make one final comparison to experiment. Pasto used temperature-dependent results for rate constants to compute an activation energy $E_a = \Delta^\ddagger H^\circ + RT = 9 \text{ kcal mol}^{-1}$, and activation entropy $\Delta^\ddagger S^\circ = -27 \text{ eu}$, for the reaction of $\text{BH}_3 \cdot \text{THF}$ adducts with tetramethylethene.³ His E_a disagrees substantially with ours (14.7 or $21.8 \text{ kcal mol}^{-1}$ for S_N2 or S_N1 mechanisms, respectively). Since the comparisons so far suggest that our accuracy is within 2 kcal mol^{-1} , we conclude that something is wrong in the experimental value. Singleton suspected problems with the temperatures reported for the rate constants.¹¹ However, there might be problems with the temperature dependence of the Eyring equation itself; we had problems reproducing an Eyring-determined $\Delta^\ddagger S^\circ$ value for a permanganate reaction,⁴⁴ and Brown noted historical problems in using Eyring-determined $\Delta^\ddagger S^\circ$ values for understanding mechanism.²

4. CONCLUSIONS

The nature of boranes in solution (monomer, dimer, or solvent adduct) can be monitored with ^{11}B -NMR or infrared measurements, as the Brown group² did. Our calculations confirm that monomer peaks would appear in noticeably different locations in both spectra.

The entropy-damping (system-frame) procedures introduced here appear to improve upon the concentrated-gas (molecule-frame) method (comparisons 3 and 4 and application 1, $(9\text{BBN})_2$ dissociation vs solvolysis). Based only on the tests performed here, we appear to have achieved 2 kcal mol^{-1} accuracy in these systems, but for rate constants this still allows for errors of a factor of 30. Because of this, our improvements were not sufficient to verify all of Brown's hypotheses for hydroboration in THF solvent. The calculations showed that the solvolysis stage is S_N2 (to SBB intermediate) + S_N1 (to 2 SB) for B_2H_6 , but could not confirm this for $(9\text{BBN})_2$, and they showed that the alkene addition stage is $S_N1 + 4e$ rearrangement for $9\text{BBN} \cdot \text{THF}$, but could not confirm this for $\text{BH}_3 \cdot \text{THF}$.

Differences between $\Delta_{\text{rxn}}H$ and $\Delta_{\text{rxn}}G$ in THF solution are significant (see the Supporting Information), and continuum-solvation methodologies could be improved to address this.

■ APPENDIX A: INTERNAL ROTATION ENTROPY TESTS

We tested the harmonic-oscillator (HO) entropy estimate for the nine internal rotation modes that we thought might be least hindered. E1 theory²⁸ required us to compute MP2/6-31G(d) internal-rotation barrier heights, and to replace S^{HO} with S^{free} free-rotor results if the MP2/6-31G(d) barriers were less than $1.4RT = 3.5 \text{ kJ mol}^{-1}$. Table 8 shows that the S^{HO} value is sufficiently accurate, even in the cases where E1 theory recommends replacement with S^{free} , and so no replacements were done. The largest error we made by keeping S^{HO} values would be in the first case of Table 8: by keeping $(16.6 + 11.3)/2$ instead of using 16.1, we make an error of $2.1 \text{ J mol}^{-1} \text{ K}^{-1}$ in S , or an error of $0.2 \text{ kcal mol}^{-1}$ in TS or G .

■ APPENDIX B: VARIATIONAL TRANSITION-STATE EFFECTS

Accurate computation of activation free energies $\Delta^\ddagger G$ ($G^\ddagger - G_{\text{reactants}}$) are needed to predict rates via Eyring-equation rate constants k :

$$k = \kappa Q^\circ \frac{k_B T}{h} e^{-\Delta^\ddagger G^\circ / RT}$$

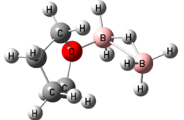
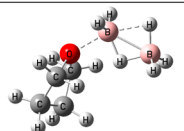
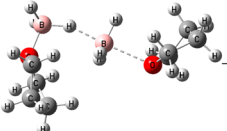
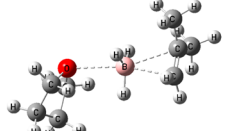
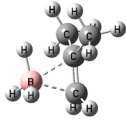
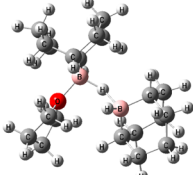
where k_B is Boltzmann's constant, h is Planck's constant, κ is the recrossings factor, and Q° is the reaction quotient of standard concentrations, $[\text{transition state}]/[\text{reactant(s)}]$, i.e. in solution normally Q° is 1 for unimolecular reactions and 1 M^{-1} for bimolecular reactions. The challenging goal of reducing uncertainty in $\Delta^\ddagger G$ prediction in solution to 2 kcal mol^{-1} would reduce inaccuracies in k to a factor of 30. Due to this limited accuracy, (i) we set $\kappa = 1$, because the error in neglecting recrossings is likely to be swamped by the error in $\Delta^\ddagger G$, and (ii) we focused on determining values for $\delta_{\text{FES}}G$ (the sum of terms 7 and 8 in Table 1) only for the free energy of transition states of barrierless reactions (for which the terms might be largest).

We first computed gas-phase values for $\delta_{\text{FES}}G$, with the intent of adding solvation corrections later. The gas-phase values were determined by performing partial geometry optimizations at various fixed values of interfragment distance ($R_{\text{B-O}}$ for adduct dissociation, $R_{\text{B-B}}$ for diborane dissociation), computing an ideal-gas RRHO-based Gibbs energy after each optimization, plotting these $G_{\text{gas,init}}(R)$ values, and taking the maximum value to be G^\ddagger . Table 9 shows some results.

Before adding solvation corrections to these, we first compared to an experimental value for the gas-phase reaction $2\text{BH}_3 \rightarrow \text{B}_2\text{H}_6$, derived as follows. Mappes and co-workers⁴⁵ performed experiments and used a Slater extrapolation to determine a high-pressure-limit second-order rate constant of $k_2 = 10^{10.6 \pm 0.4}$ at $T = 545 \text{ K}$. Using $k = Ae^{E_a/RT}$ and a plot of $\ln k$ vs $1/T$ they determined that $E_a = -1 \pm 2 \text{ kcal mol}^{-1}$. This gives $A = 10^{10.3}$; using this A and E_a but with $T = 298 \text{ K}$ one finds $k_2(298\text{K}) = 10^{11.0}$. Equating this with the Eyring equation above, one derives $\Delta^\ddagger G^\circ = 2.4 \text{ kcal mol}^{-1}$. (Since $\Delta^\ddagger H^\circ = E_a - 2RT$ for a bimolecular reaction, $\Delta^\ddagger H^\circ = -2.2 \text{ kcal mol}^{-1}$, leaving $T\Delta^\ddagger S^\circ = -4.6 \text{ kcal mol}^{-1}$. The uncertainties in $\Delta^\ddagger G^\circ$, $\Delta^\ddagger H^\circ$, and $T\Delta^\ddagger S^\circ$ are slightly greater than 2 kcal mol^{-1} .) In comparison to this experimental result for BH_3 dimerization, we overpredict $\Delta^\ddagger G^\circ$ (5.8 , versus 2.4 ± 2). This could be due to an overly low HO-based estimate of S^* , causing our $T\Delta^\ddagger S^\circ$ (-7.0 , versus -4.6 ± 2) to be too large a drop; anharmonic effects should bring this value into better agreement with experiment. (A more elaborate prediction of $\Delta^\ddagger G^\circ$, for the $2\text{CH}_3 \rightarrow \text{C}_2\text{H}_6$ reaction, gave $\Delta^\ddagger G^\circ = 3 \text{ kcal mol}^{-1}$,⁴⁶ matching this value for 2BH_3 from experiment, but this procedure may not be possible for our largest molecule.)

The poor agreement in the gas phase led us to discard Table 9 results and instead add solvation corrections to the experimental gas-phase values of $\{+2.4, -2.2, -4.6\} \text{ kcal mol}^{-1}$ for $\{\Delta^\ddagger G^\circ, \Delta^\ddagger H^\circ, T\Delta^\ddagger S^\circ\}$ for barrierless associations. For solvation corrections (terms I–IX in Table 1), we assumed that term II (polarization) does not appreciably change during the approach of two molecules to the loose variational transition state, and focused on damping terms. Damping PV (by $-RT$ on the transition state and $-2RT$ on the fragments) adds $+0.6$ to $\Delta^\ddagger H$, while damping TS (by 25% of TS_{gas} for both the transition state and the fragments, since this reproduces the computed damping on the fragments) will

Table 8. Entropy S of Internal Rotation Modes, from MP2/6-31G(d) Optimizations

System	Mode	Barrier (kJ mol ⁻¹)	S^{HO} (J mol ⁻¹ K ⁻¹)	S^{free} (J mol ⁻¹ K ⁻¹)	$I^{(2,1)a}$ (amu Å ²)
	BH ₃ spin	2.9	16.6 or 11.3 ^b	16.1	4.0924
	H _{bridge} revolution	7.8	Fine ^c		
	B-O torsion	11.8	Fine		
	BH ₃ spin (ratchet)	≤3.3	16.6 or 12.8 ^b	16.3	4.3004
	Heavy end-end torsion	≥5.4	Fine		
	BH ₃ spin	1.0	17.1	16.2	4.2416
	B-O end-end torsion	1.5	40.4	38.1	91.9154
	BH ₃ spin	7.3	Fine		
	B-B torsion	>9.5 ^d	Fine		

^aReduced moment of inertia for internal rotation.²⁸ ^bTwo normal modes share internal rotation character; in such a case one might consider replacing their average contribution with a free-rotor contribution. ^c"Fine": The harmonic oscillator prediction would not need replacing according to E1 theory.²³ ^dB3LYP/6-31G(d) result.

Table 9. Results from Variational Transition-State Partial Optimizations

reaction	method	basis set	$R^\ddagger/\text{\AA}^a$	$\Delta^\ddagger G(\text{gas})/\text{kcal mol}^{-1}$
2 9BBN → (9BBN) ₂	B3LYP	6-31G(d)	3.0	11.0 ^b
2 9BBN → (9BBN) ₂	MP2	6-31G(d)	4.0	6.6 ^b
2 BH ₃ → B ₂ H ₆	MP2	6-31G(d)	3.0	5.8 ^c
BH ₃ + THF → BH ₃ THF	B3LYP	aug-cc-pVDZ	3.5	4.6
BH ₃ + NH ₃ → BH ₃ NH ₃	B3LYP	aug-cc-pVDZ	4.0	3.8
BH ₃ + NH ₃ → BH ₃ NH ₃	B3LYP	6-31G(d)	4.5	3.7

^a $R(\text{B}-\text{B})$ for the first 3 rows; $R(\text{B}-\text{O})$ for the 4th row; $R(\text{B}-\text{N})$ for the last 2 rows. ^bRather large estimates for 9BBN dimerization may be due to increased error in the HO approximation, caused by frequencies lowered by the large mass of the system. ^cExperimental result is $2.4 \pm 2 \text{ kcal mol}^{-1}$ (see text).

add $-0.25 T\Delta^\ddagger S_{\text{gas}} = +1.2$ to $T\Delta^\ddagger S$. This resulted in solution-phase values of $\{+1.8, -1.6, -3.4\} \text{ kcal mol}^{-1}$ for $\{\Delta^\ddagger G^\circ, \Delta^\ddagger H^\circ, T\Delta^\ddagger S^\circ\}$ for barrierless associations in THF. Hence, these values were used as $\{\delta_{\text{FES}}G, \delta_{\text{FES}}E = \delta_{\text{FES}}H, \delta_{\text{FES}}TS\}$ for S_N1 barrierless dissociations in THF solution.

■ ASSOCIATED CONTENT

■ Supporting Information

Figure S1 showing predicted IR spectra, B3LYP/6-31G(d); Figure S2 showing lowest-energy conformations of the THF adducts of B₂H₆ and (9-BBN)₂; two energy tables; one table of S_{rot} parameter values; and Cartesian coordinates of all B3LYP/6-31G(d) structures. This material is available free of charge via the Internet at <http://pubs.acs.org>.

■ AUTHOR INFORMATION

Corresponding Author

*E-mail: allan.east@uregina.ca. Tel: 306-585-4003.

Notes

The authors declare no competing financial interest.

■ ACKNOWLEDGMENTS

We gratefully acknowledge NSERC (Canada) for operational grant funding and the Canada Foundation for Innovation, Government of Saskatchewan, and CiaraTech (Canada) for supercomputer funding. The Laboratory of Computational Discovery (John Jorgensen and Robert Cowles, sysadmins) is thanked for supercomputer upkeep. Arumugam Jayaraman and Chatin Bains are thanked for assistance in particular

computational transition-state searches. Stephen Klippenstein (Argonne) is thanked for a discussion of barrierless reactions in solution.

REFERENCES

- (1) Burkhardt, E. R.; Matos, K. Boron Reagents in Process Chemistry: Excellent Tools for Selective Reductions. *Chem. Rev.* **2006**, *106*, 2617–2650.
- (2) Wang, K. K.; Brown, H. C. Hydroboration Kinetics. 6. Hydroboration of Alkenes with 9-Borabicyclo[3.3.1]nonane Dimer and 9-Borabicyclo[3.3.1]nonane-Lewis Base Complexes in Various Solvents: An Interpretation of the Catalytic Effect of Ether Solvents on the Hydroboration Reaction. *J. Am. Chem. Soc.* **1982**, *104*, 7148–7155.
- (3) Pasto, D. J.; Lepeska, B.; Cheng, T. C. Transfer Reactions Involving Boron. XXIV. Measurement of the Kinetics and Activation Parameters for the Hydroboration of Tetramethylethylene and Measurement of Isotope Effects in the Hydroboration of Alkenes. *J. Am. Chem. Soc.* **1972**, *94*, 6083–6090.
- (4) Pasto, D. J.; Lepeska, B.; Balasubramanian, V. Transfer Reactions Involving Boron. XXV. Measurement of the Relative Rate Ratios of the First and Second Steps of the Hydroboration Reaction and the Rates of Alkylborane Redistribution Reactions. Discussion of the Overall Mechanism of the Hydroboration Reaction. *J. Am. Chem. Soc.* **1972**, *94*, 6090–6096.
- (5) Brown, H. C.; Chandrasekharan, J. Mechanism of Hydroboration of Alkenes with Borane-Lewis Base Complexes. Evidence that the Mechanism of the Hydroboration Reaction Proceeds through a Prior Dissociation of such Complexes. *J. Am. Chem. Soc.* **1984**, *106*, 1863–1865.
- (6) McKee, M. L. Ab Initio Study of the Formation of Aminoborane from Ammonia and Diborane. *J. Phys. Chem.* **1992**, *96*, 5380–5385.
- (7) Mebel, A. M.; Musaev, D. G.; Morokuma, K. Ab Initio Molecular Orbital Study of Mechanisms of the Reaction of Diborane with Hydrogen Sulfide. *J. Phys. Chem.* **1993**, *97*, 7543–7552.
- (8) McKee, M. L. Ab Initio Study of Diborane Hydrolysis. *J. Phys. Chem.* **1996**, *100*, 8260–8267.
- (9) Clark, T.; Wilhelm, D.; Schleyer, P. v. R. Mechanism of Hydroboration in Ether Solvents. A Model Ab Initio Study. *J. Chem. Soc., Chem. Commun.* **1983**, 606–608.
- (10) Wang, X.; Li, Y.; Wu, Y.-D.; Paddon-Row, M. N.; Rondan, N. G.; Houk, K. N. Ab Initio Transition Structures for Hydroborations of Alkenes, Allenes, and Alkynes by Borane, Diborane, Methylborane, Methylfluoroborane, and Dimethylborane. *J. Org. Chem.* **1990**, *55*, 2601–2609.
- (11) Oyola, Y.; Singleton, D. A. Dynamics and the Failure of Transition State Theory in Alkene Hydroboration. *J. Am. Chem. Soc.* **2009**, *131*, 3130–3131.
- (12) Ess, D. H.; Kister, J.; Chen, M.; Roush, W. R. Quantum-Mechanical Study of 10-R-9-borabicyclo[3.3.2]decane Alkene Hydroboration. *J. Org. Chem.* **2009**, *74*, 8626–8637.
- (13) Glowacki, D. R.; Liang, C. H.; Marsden, S. P.; Harvey, J. N.; Pilling, M. J. Alkene Hydroboration: Hot Intermediates That React While They Are Cooling. *J. Am. Chem. Soc.* **2010**, *132*, 13621–13623.
- (14) Frisch, M. J.; et al., *Gaussian 09*, Revision B.01; Gaussian, Inc.: Wallingford, CT, 2009.
- (15) Becke, A. D. Density-Functional Thermochemistry. III. The Role of Exact Exchange. *J. Chem. Phys.* **1993**, *98*, 5648–5652.
- (16) Lee, C.; Yang, W.; Parr, R. G. Development of the Colle-Salvetti Correlation-Energy Formula into a Functional of the Electron Density. *Phys. Rev. B* **1988**, *37*, 785–789.
- (17) Perdew, J. P.; Burke, K.; Ernzerhof, M. Generalized Gradient Approximation Made Simple. *Phys. Rev. Lett.* **1996**, *77*, 3865–3868.
- (18) Perdew, J. P.; Burke, K.; Ernzerhof, M. Erratum: Generalized Gradient Approximation Made Simple. *Phys. Rev. Lett.* **1997**, *78*, 1396.
- (19) Handy, N. C.; Cohen, A. J. Left-Right Correlation Energy. *J. Mol. Phys.* **2001**, *99*, 403–412.
- (20) Rayon, V. M.; Sordo, J. A. Pseudorotation Motion in Tetrahydrofuran: An Ab Initio Study. *J. Chem. Phys.* **2005**, *122*, 204303.
- (21) Wolinski, K.; Hinton, J. F.; Pulay, P. Efficient Implementation of the Gauge-Independent Atomic Orbital Method for NMR Chemical Shift Calculations. *J. Am. Chem. Soc.* **1990**, *112*, 8251–8260.
- (22) Cheeseman, J. R.; Trucks, G. W.; Keith, T. A.; Frisch, M. J. A Comparison of Models for Calculating Nuclear Magnetic Resonance Shielding Tensors. *J. Chem. Phys.* **1996**, *104*, 5497–5509.
- (23) East, A. L. L.; Allen, W. D. The Heat of Formation of NCO. *J. Chem. Phys.* **1993**, *99*, 4638–4650.
- (24) Allen, W. D.; Császár, A. G. The Composite Focal-Point Analysis (FPA) Approach. In *Molecular Quantum Mechanics: From Methylene to DNA and Beyond*; Bartlett, R. J.; Crawford, T. D.; Head-Gordon, M.; Sherrill, D. C., Eds.; Brandon's Printing: Atlanta, GA, 2010.
- (25) Hampel, C.; Peterson, K.; Werner, H.-J. A Comparison of the Efficiency and Accuracy of the Quadratic Configuration Interaction (QCISD), Coupled Cluster (CCSD), and Brueckner Coupled Cluster (BCCD) Methods. *Chem. Phys. Lett.* **1992**, *190*, 1–12.
- (26) Werner, H.-J.; Knowles, P. J.; Lindh, R.; Manby, F. R.; Schütz, M.; Celani, P.; Korona, T.; Mitrushenkov, A.; Rauhut, G.; et al. *MOLPRO 2008.1 program*; Cardiff University: Cardiff, U.K., 2008.
- (27) Merrick, J. P.; Moran, D.; Radom, L. An Evaluation of Harmonic Vibrational Frequency Scale Factors. *J. Phys. Chem. A* **2007**, *111*, 11683–11700.
- (28) East, A. L. L.; Radom, L. Ab Initio Statistical Thermodynamic Models for the Computation of Third-Law Entropies. *J. Chem. Phys.* **1997**, *106*, 6655–6674.
- (29) Guthrie, J. P. Use of DFT Methods for the Calculation of the Entropy of Gas Phase Organic Molecules: An Examination of the Quality of Results from a Simple Approach. *J. Phys. Chem. A* **2001**, *105*, 8495–8499.
- (30) Khalili, F.; Henni, A.; East, A. L. L. Entropy Contributions in pK_a Computation: Application to Alkanolamines, and Piperazines. *J. Mol. Struct.: THEOCHEM* **2009**, *916*, 1–9.
- (31) Truhlar, D. G.; Garrett, B. C. Variational Transition-State Theory. *Acc. Chem. Res.* **1980**, *13*, 440.
- (32) Tomasi, J.; Mennucci, B.; Cammi, R. Quantum Mechanical Continuum Solvation Models. *Chem. Rev.* **2005**, *105*, 2999–3093.
- (33) Scalmani, G.; Frisch, M. Continuous Surface Charge Polarizable Continuum Models of Solvation. I. General Formalism. *J. Chem. Phys.* **2010**, *132*, 114110.
- (34) Amzel, L. M. Loss of Translational Entropy in Binding, Folding, and Catalysis. *Proteins* **1997**, *28*, 144–149.
- (35) Irudayam, S. J.; Henschman, R. H. Entropic Cost of Protein-Ligand Binding and Its Dependence on the Entropy in Solution. *J. Phys. Chem. B* **2009**, *113*, 5871–5884.
- (36) Wertz, D. H. Relationship Between the Gas-Phase Entropies of Molecules and their Entropies of Solvation in Water and 1-Octanol. *J. Am. Chem. Soc.* **1980**, *102*, 5316–5322.
- (37) Hildebrand, J. H. Liquid Structure and Entropy of Vaporization. *J. Chem. Phys.* **1939**, *7*, 233–235.
- (38) Nash, L. K. Trouton and T-H-E Rule. *J. Chem. Educ.* **1984**, *61*, 981–984.
- (39) Marenich, A. V.; Cramer, C. J.; Truhlar, D. G. Universal Solvation Model Based on Solute Electron Density and on a Continuum Model of the Solvent Defined by the Bulk Dielectric Constant and Atomic Surface Tensions. *J. Phys. Chem. B* **2009**, *113*, 6378–6396.
- (40) Sumon, K. Z.; Henni, A.; East, A. L. L. Predicting pK_a of Amines for CO₂ Capture: Computer versus Pencil-and-Paper. *Ind. Eng. Chem. Res.* **2012**, *51*, 11924–11930.
- (41) Ben-Naim, A. *Molecular Theory of Solutions*; Oxford University Press: Oxford, UK, 2006.
- (42) Ewing, G. E. Spectroscopic Studies of Molecular Motion in Liquids. *Acc. Chem. Res.* **1969**, *2*, 168–174.

- (43) Brown, H. C.; Scouten, C. G.; Wang, K. K. Unusual Kinetics for the Hydroboration of Alkenes with 9-Borabicyclo[3,3,1]nonane. *J. Org. Chem.* **1979**, *44*, 2589–2591.
- (44) Jayaraman, A.; East, A. L. L. The Mechanism of Permanganate Oxidation of Sulfides and Sulfoxides. *J. Org. Chem.* **2012**, *77*, 351–356.
- (45) Mappes, G. W.; Fridmann, S. A.; Fehlner, T. P. Absolute Rate of Association of Borane Molecules. *J. Phys. Chem.* **1970**, *74*, 3307–3316.
- (46) de Sainte Claire, P.; Peslherbe, G. H.; Wang, H.; Hase, W. L. Linear Free Energy of Activation Relationship for Barrierless Association Reactions. *J. Am. Chem. Soc.* **1997**, *119*, 5007–5012.